A systematic evaluation of pre-trained encoder architectures for multimodal brain tumor segmentation using U-Net-based architectures

Marwa Abbas¹, Ashraf A. M. Khalaf², Hussein Mogahed¹, Aziza I. Hussein³, Lamya Gaber¹, M. Mourad Mabrook⁴

¹Department of Computer and Systems Engineering, Faculty of Engineering, Minia University, Al-Minia, Egypt

²Department of Electronics and Communications Engineering, Faculty of Engineering, Minia University, Al-Minia, Egypt

³Electrical and Computer Engineering Department, Effat University, Jeddah, Arab Saudi

⁴Space Communication Department, Faculty of Navigation Science and Space Technology, Beni-Suef University, Beni-Suef, Egypt

Article Info

Article history:

Received Jan 19, 2025 Revised Jul 28, 2025 Accepted Oct 14, 2025

Keywords:

Brain tumor cancer Encoders Medical imaging Pre-trained U-Net segmentation

ABSTRACT

Accurate brain tumor segmentation from medical imaging is critical for early diagnosis and effective treatment planning. Deep learning methods, particularly U-Net-based architectures, have demonstrated strong performance in this domain. However, prior studies have primarily focused on limited encoder backbones, overlooking the potential advantages of alternative pretrained models. This study presents a systematic evaluation of twelve pretrained convolutional neural networks ResNet34, ResNet50, ResNet101, VGG16, VGG19, DenseNet121, InceptionResNetV2, MobileNetV2, EfficientNetB1, SE-ResNet34, and SE-ResNet18—used as encoder backbones in the U-Net framework for identification and extraction of tumor-affected brain areas using the BraTS 2019 multimodal MRI dataset. Model performance was assessed through cross-validation, incorporating fault detection to enhance reliability. The MobileNetV2-based U-Net configuration outperformed all other architectures, achieving 99% cross-validation accuracy and 99.3% test accuracy. Additionally, it achieved a Jaccard coefficient of 83.45%, and Dice coefficients of 90.3% (Whole Tumor), 86.07% (Tumor Core), and 81.93% (Enhancing Tumor), with a low-test loss of 0.0282. These results demonstrate that MobileNetV2 is a highly effective encoder backbone for U-Net in extracting tasks for tumor-affected brain regions using multimodal medical imaging data.

This is an open access article under the CC BY-SA license.



850

Corresponding Author:

Marwa Abbas

Department of Computer and Systems Engineering, Faculty of Engineering, Minia University Al-Minia, 61111, Egypt

Email: Marwa.abas@mu.edu.eg

1. INTRODUCTION

Brain tumors, defined by aberrant neural cell proliferation, constitute one of the most difficult problems in neuro-oncology, with significant global incidence (e.g., 23,820 new cases reported in the US in 2019 [1], [2]). Accurate diagnosis and management of these tumors rely heavily on advanced medical imaging modalities, particularly multiparametric MRI (T1, T1c, T2, FLAIR), which provides superior soft-tissue contrast for delineating tumor boundaries compared to CT or ultrasound [3], [4]. While these imaging techniques are indispensable, manual segmentation of tumor subregions (enhancing tumor, necrotic core, and peritumoral edema) remains labor-intensive, time-consuming, and subject to inter-rater variability, underscoring the critical need for automated, high-precision computational methods.

Journal homepage: http://ijeecs.iaescore.com

Traditional machine learning approaches for brain tumor segmentation often struggle with limited feature generalizability and dependence on handcrafted feature engineering. In contrast, deep learning (DL), particularly convolutional neural networks (CNNs), has shown powerful success in medical image analysis through autonomous acquisition of hierarchical features. Among DL architectures, U-Net has emerged as the de facto standard for biomedical segmentation, utilizing an encoder-decoder configuration combined with skip connections, which help maintain spatial details during the learning process [5], [6]. However, U-Net implementations face challenges, including high computational complexity and dependence on sizable annotated datasets, a major obstacle in the domain of medical imaging due to the scarcity of labeled data.

To address these limitations, transfer learning (TL) has been increasingly adopted, employing pretrained CNNs (e.g., ResNet, VGG, DenseNet) as encoders to enhance feature extraction while reducing training time [7], [8]. Recent studies highlight the efficacy of TL-integrated U-Net variants.

Nawaz et al. [9] achieved 0.81–0.88 Dice similarity coefficient for tumor subregions using VGG19-U-Net. While Ghosh et al. [10] have suggested a k-fold cross-validation method and U-Net architecture employing VGG-16 as a backbone network for segmenting brain tumors. Their model achieved a 92% Dice score on the TCGA-LGG dataset. Lin et al. [11] reported improved efficiency with EfficientNetV2-U-Net for multi-sequence MRI. Rabby et al. [12] attained an 86% Dice score using InceptionV3-U-Net, while 3D extensions further improved multi-modal fusion. Saifullah et al. [13] suggested a combined model that integrates ResNet50 with DeepLabV3, achieving a 96.9% Dice score on the Figshare dataset. Authors in [14]. Proposed a framework that utilizes the EfficientNetB4 as its feature extraction backbone. EfficientNetB4 employs a method of mixture scaling that enhances the network's width, depth, and resolution to get a good balance between performance and computational efficiency. Their model scored 93.39% Dice score on the Figshare dataset. Another study [15] presents a custom approach using Convolutional Neural Networks (CNNs) with DenseNet201 to detect and categorize Acute lymphoblastic leukaemia cases using 3562 blood smear images from 89 patients, achieving 98% segmentation accuracy and 97.09% test accuracy.

Despite these advances, a systematic comparison of pre-trained encoders for brain tumor segmentation remains underexplored, particularly regarding their computational efficiency, segmentation accuracy, and ability to generalize across tumor categories.

This study presents a comprehensive evaluation of 12 pre-trained CNN architectures as U-Net encoders for multimodal brain tumor segmentation, using the BraTS 2019 dataset. Key innovations include:

- a) Architectural Benchmarking: Precise comparison of ResNet34/50/101, VGG16/19, DenseNet121, InceptionResNetV2/V3, MobileNetV2, and EfficientNetB1, quantifying performance via Dice, Jaccard, and computational metrics.
- b) Novel SE-ResNet Integration, which utilizes squeeze-and-excitation blocks to improve feature extraction, SE-ResNet18/34 was first used as U-Net encoders.
- Computational-accuracy trade-off analysis: Identification of MobileNetV2 as an optimal encoder, balancing accuracy and efficiency.

This manuscript's sections are prepared as follows: Section 2 demonstrates the suggested framework and various frameworks employed in the research, along with implementation specifics and assessment criteria. Section 3 outlines the outcomes and subsequent analysis for twelve pre-trained encoders. Section 4 illustrates the conclusion of this work.

2. METHOD

The experimental methodology used in this study is explained in this section. Initially, a publicly accessible multimodal MRI BraTS 2019 dataset was selected. A sequence of preprocessing steps was used to ensure compatibility with the deep learning models. These transformations standardized the image dimensions to 224x224 pixels, including rotation and contrast adjustment. Following data preprocessing, the chosen deep learning models were implemented, and their performance was subsequently evaluated using relevant metrics. Additionally, this section offers a thorough explanation of the dataset, a brief examination of the deep learning architectures that have been applied in execution, and an inclusive evaluation of the performance of the proposed approach.

2.1. Standard U-Net model

The U-Net architecture [16], created for the segmentation of biomedical images, is a fully convolutional network (FCN) distinguished by its unique U-shaped topology. There are two main parts to this architecture:

a) Contextual information and abstract features are captured by the Contracting Path (Encoder), which gradually downsamples the input image. Convolutional layers are applied repeatedly, and then pooling operations are performed.

b) The expanding path (Decoder) improves spatial resolution by upsampling feature maps from the contracting path and using skip connections to merge low spatial resolution contextual information with high spatial resolution localized features, as presented in Figure 1.

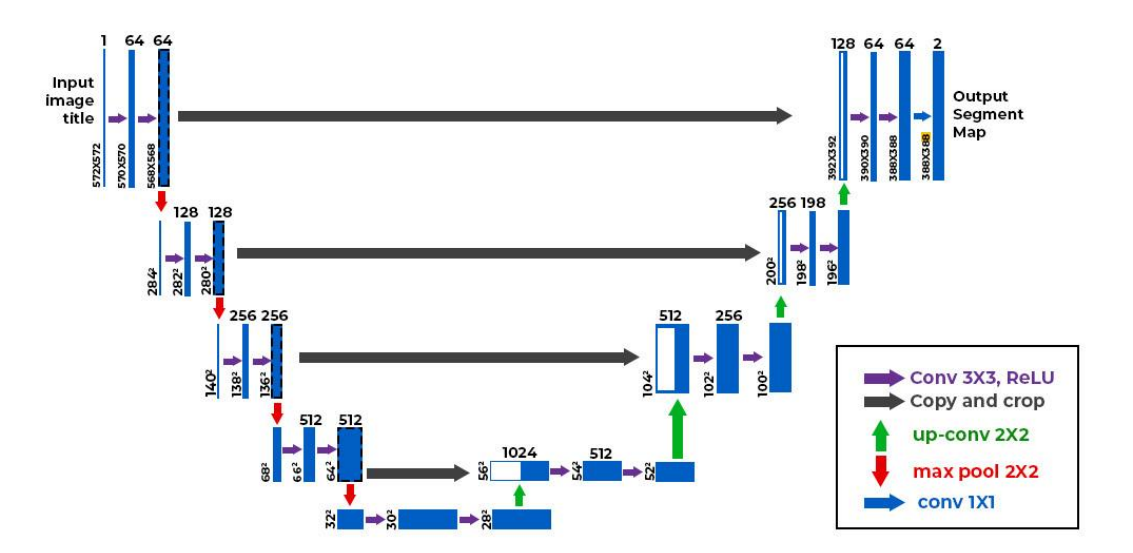


Figure 1. U-net model structure visualization

2.2. Proposed models for encoders

This framework involves an upsampling path (decoder) intended to restore spatial resolution and improve the segmentation output, and a downsampling path (encoder) responsible for feature extraction. Initially, the decoder component within the U-Net architecture was held constant, while the encoder component was replaced with pre-trained models. The proposed study utilized 12 pre-trained encoder algorithms, including ResNet34, ResNet50, ResNet101, VGG16, VGG19, DenseNet121, InceptionResNetV2, Inception V3, MobilenetV2, Efficient Net B1, SE ResNet34, and SE ResNet18 as encoders with the fixed decoder part in the U-Net architecture only. Figure 2 presents a comprehensive description of the research workflow, and Table 1 compares pre-trained encoders in terms of the number of layers.

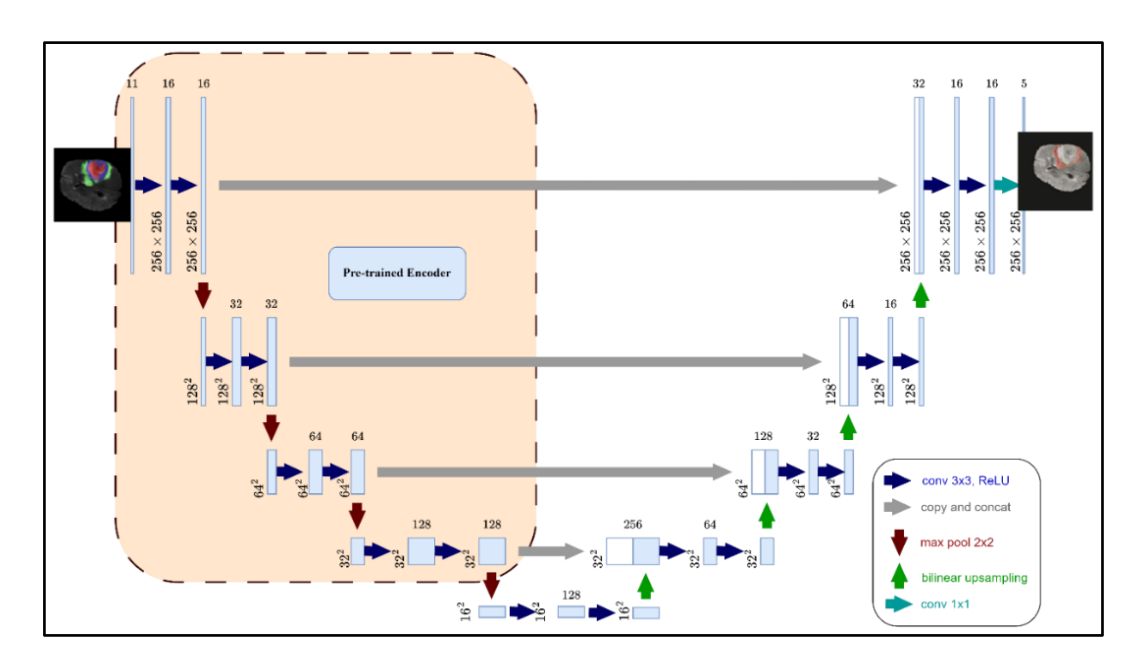


Figure 2. Overview of the investigation's workflow

П

Model	Number of Layers		
DenseNet-121	121		
ResNet34	34		
ResNet50	50		
ResNet101	101		
VGG16	16		
VGG19	19		
Inception-v3	48		
Inception-ResnetV2	164		
SE ResNet18	183		
SE ResNet34	311		
Efficient Net B2	373		
MobilenetV2	196		

Table 1. Comparison of pre-trained encoders in terms of number of layers

ImageNet weights were used to initialize these backbone encoders, and the encoder layers were all kept frozen. Then, the 12 pre-trained encoders were trained on the specific dataset to generate their models. The procedures that compose the training phase are explained in Algorithm 1.

Algorithm 1. Steps (Training Phase)

Step 1: Brain MRI images are read from the selected dataset.

Step 2: The images are resized to match the input dimensions required by the transfer learning models.

Step 3: The dataset is distributed into 70% for training, 10% for validation, and 20% for testing.

Step 4: Features are extracted from each of the twelve models pre-trained on the benchmark dataset.

Step 5: Adjusting and optimizing the associated function to train pre-trained models.

Step 6: Fully trained models are generated.

2.3. The input dataset

This study uses twelve pre-trained models as backbone encoders in an experimental study using the MICCAI BraTS 2019 [17] challenge dataset with 335 cases. The dataset includes native, post-contrast, T2-weighted, and T2-FLAIR scan volumes. The study identifies necrotic and non-enhancing tumor core NCR/NET (label 1), peritumoral edema ED, and enhancing tumor ET labels, transforming them into 3-channel volumes. Each imaging dataset segments three labels. The illustration in Figure 3 displays four different modalities and the mask.

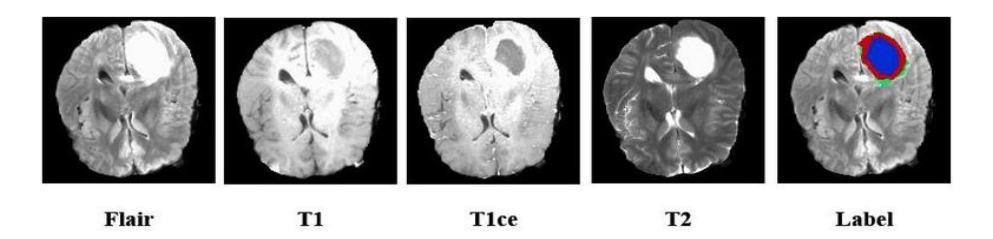


Figure 3. BraTS 2019 modalities and generated mask

2.4. Training and experimental configuration

Model training was conducted using an Nvidia Tesla P100 GPU with 16GB GDDR6 VRAM. The framework used in the experiments is TensorFlow. The dataset's distribution is 80% chosen at random for training (70% for training and 10% for validation), with the remaining 20% going toward testing. While training, the optimizer Adam is used with a learning rate value set at 0.0001 [18] and Relu for activation function with 50 epochs. The loss function that is utilized is binary_ cross-entropy. The definition of binary-cross-entropy [19] is shown in (1).

$$L_c = -\frac{1}{n} \sum_{i=1}^{n} \{ y_i \log f_i + (1 - y_i) \log (1 - f_i) \}$$
 (1)

2.5. Evaluation metrics

For model evaluation, by dividing the total number of predictions by the sum of accurate positive and negative predictions, the accuracy score is determined as in (2). Another metrics are the Dice coefficient and the Jaccard coefficient, which can be calculated according to (3) and (4).

$$Accuracy = \frac{TP + TN}{TP + TN + FN + FP} \tag{2}$$

$$Dice\ Cofficent = \frac{2TP}{2TP + FP + FN} \tag{3}$$

$$Jaccard\ Cofficent = \frac{TP}{TP + FP + FN} \tag{4}$$

3. RESULTS AND DISCUSSION

The suggested study used pre-trained deep learning architectures as an encoder backbone for Unet to segment brain tumors from multimodal MRI images with ImageNet weights. Here, 12 pre-trained architectures are applied as encoders for Unet: ResNet34, ResNet50, ResNet101, VGG16, VGG19, DenseNet121, InceptionResNetV2, Inception V3, MobilenetV2, and Efficient Net B1, utilizing the BraTS 2019 brain tumor segmentation multimodal dataset. In addition, an evaluation of the two novel architectures, SEResNet 18 and SEResNet 34, was also conducted. The results of training and validation accuracy for pre-trained encoders are shown in Figure 4. Figure 5 evaluates and contrasts the pre-trained models' performance in terms of the Dice similarity coefficient. Table 2 compares pre-trained encoders for U-net models regarding training time, trainable parameters, and non-trainable parameters. The test loss and accuracy graphs for 12 different models using pre-trained encoders are compared in Figure 6. Table 3 compares the Jaccard and Dice coefficients for segmenting brain tumors with U-net with previous work.

3.1. Results analysis

According to the results in MobilenetV2 (Figure 4(I)) was the most accurate and least loss pretrained model used to segment brain tumors from the multimodal dataset (Figures 4(a)-4(c)). Followed by VGG16 and VGG19 as shown in Figures 4(d) and 4(e). Efficient Net B1 came in third place, as shown in Figure 4(k), followed by Dense121 network encoders as in Figure 4(h). InceptionResNetV2 and Inception V3 (Figure 4(f)) were also considered, but Inception V3 (Figure 4(f)) was superior in loss. ResNet34 (Figure 4(g))was considered the best of the three ResNet models (ResNet34, ResNet50, and ResNet101), while SEResNet 18 (Figure 4(i)) and SEResNet 34 (Figure 4(j)) had the worst results.

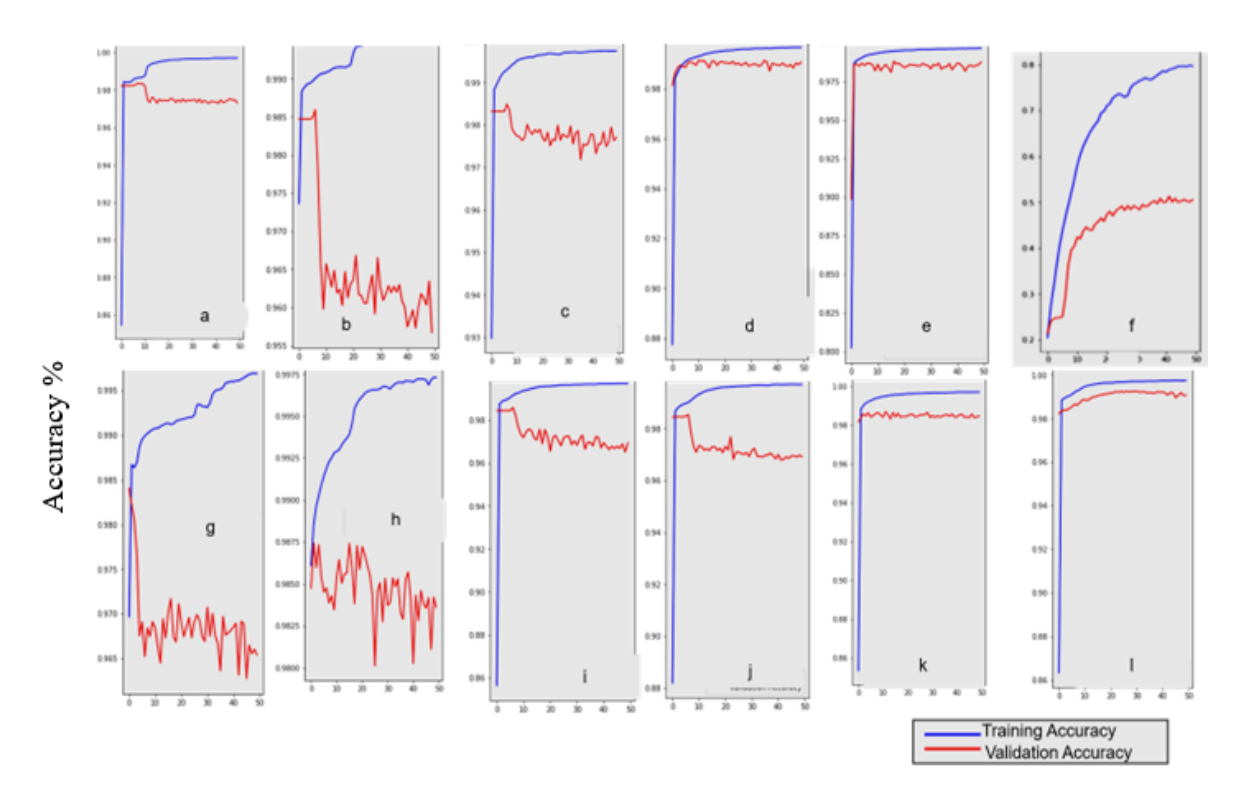
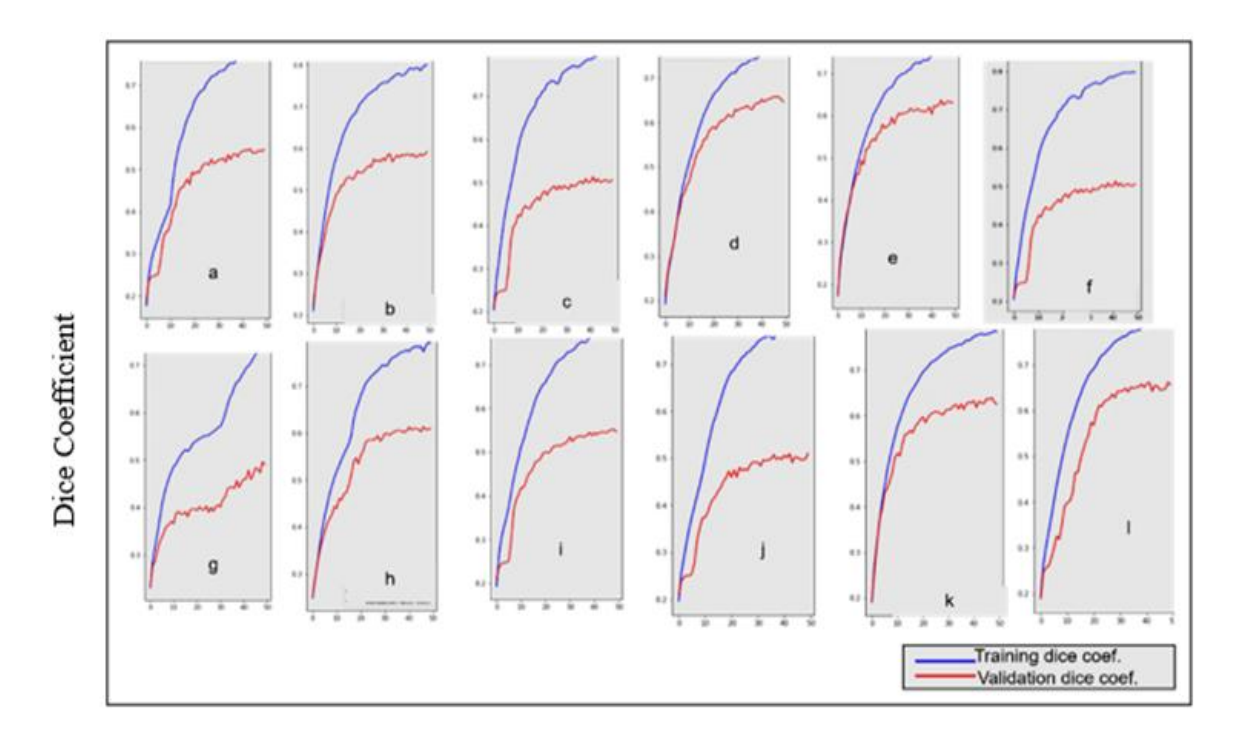


Figure 4. Training and validation accuracy: (a) ResNet34, (b)ResNet-50, (c) ResNet-101, (d) VGG16, (e) VGG19, (f) InceptionV3, (g) Inception ResNet, (h) Dense121, (i) SEResNet 18, (j) SEResNet 34, (k) Efficient Net B1 and (l) MobilenetV2

Concerning Figures 5(a)-5(l), the U-Net segmentation model utilizing MobileNetV2 as its encoder backbone had the highest dice coefficient compared to other U-Net models, as exhibited in Figure 5-1. The worst case is the Inception-Resnet-Unet model. Furthermore, Table 2 shows that the MobilenetV2-Unet achieves the minimum training time among all models with pre-trained encoders, and has the fewest parameters represented in trainable and non-trainable parameters. So, MobileNet V2 offers higher performance with fewer parameters and less computational expense than its predecessor.



Epochs

Figure 5. Training and Validation Dice coefficient: (a) ResNet-34, (b)ResNet-50, (c) ResNet-101, (d) VGG-16, (e) VGG-19, (f) InceptionV3, (g) Inception ResNet, (h) Dense121, (i) SEResNet 18, (j) SEResNet 34, (k) Efficient Net B1 and (l) MobilenetV2

Table 2. Comparison of pre-trained encoders for U-net frameworks for non-trainable parameters, trainable

Model structure	Training time	Non-trainable		
	(sec)	Total parameters (millions)	Trainable parameters	parameters
ResNet34- Unet	3199.676	24,456,589	3,167,495	21,289,094
ResNet50- Unet	3756.361	32,561,549	9,059,079	23,502,470
ResNet101- Unet	4562.659	51,605,901	9,111,303	42,494,598
VGG-16-Unet	3261.144	23,752,708	9,033,988	14,718,720
VGG-19-Unet	3325.981	29,062,404	9,033,988	20,028,416
InceptionV3-Unet	3287.786	29,933,540	8,145,988	21,787,552
Inception-ResnetV2-Unet	4652.045	62,061,988	7,753,540	54,308,448
DenseNet121-Unet	3416.719	12,145,412	5,189,572	6,955,840
SE ResNet18-Unet	3400.858	14,430,085	3,160,071	11,270,014
SE ResNet34-Unet	3356.315	24,617,785	3,167,495	21,450,290
Efficient Net B2-Unet	3765.542	12,641,604	6,126,436	6,515,168
MobilenetV2-Unet	3227.675	8,047,876	5,822,020	2,225,856

As shown in Figure 6, MobilenetV2-Unet reached the highest accuracy on the test set of 99.2%, with a loss of 0.0282. The VGG19 model achieved a test accuracy of 99.19%, followed by VGG16 with 98.68% and 0.0358 and 0.0437 test losses, respectively. Within the ResNet architecture family, ResNet34 demonstrated superior performance with 98.46% test accuracy and 0.0658 test loss compared to ResNet50 and ResNet101.In addition, we presented an evaluation of the new architectures represented by SE ResNet34

and SE ResNet18 pre-trained encoders, and they achieved the lowest test accuracy with 97.26% and 95.53%. respectively. And the highest error rate among the 12 models.

Table 3 provides a comparative analysis of the previous pre-trained encoders alongside the Unet and MobileNetV2 encoders and the two novel architectures, SEResNet34 and SE ResNet18, proposed in this study. The comparison is focused on the assessment of each model's results based on multiple evaluation metrics, e.g., Jaccard, dice coefficient for enhancing tumor (ET), tumor core (TC), and whole tumor (WT). MobilenetV2-Unet has the best dice coefficient for (ET) of 81.93%, 86.07% (TC), and 90.03% (WT) and the highest Jaccard value of 81.63%. According to the results in Table 3, MobileNet V2 as an encoder demonstrates a favorable trade-off between accuracy and computational efficiency. Figure 7 graphically represents the top four performing models out of the twelve evaluated, based on the highest obtained values for accuracy, Dice similarity coefficient, and Jaccard index.

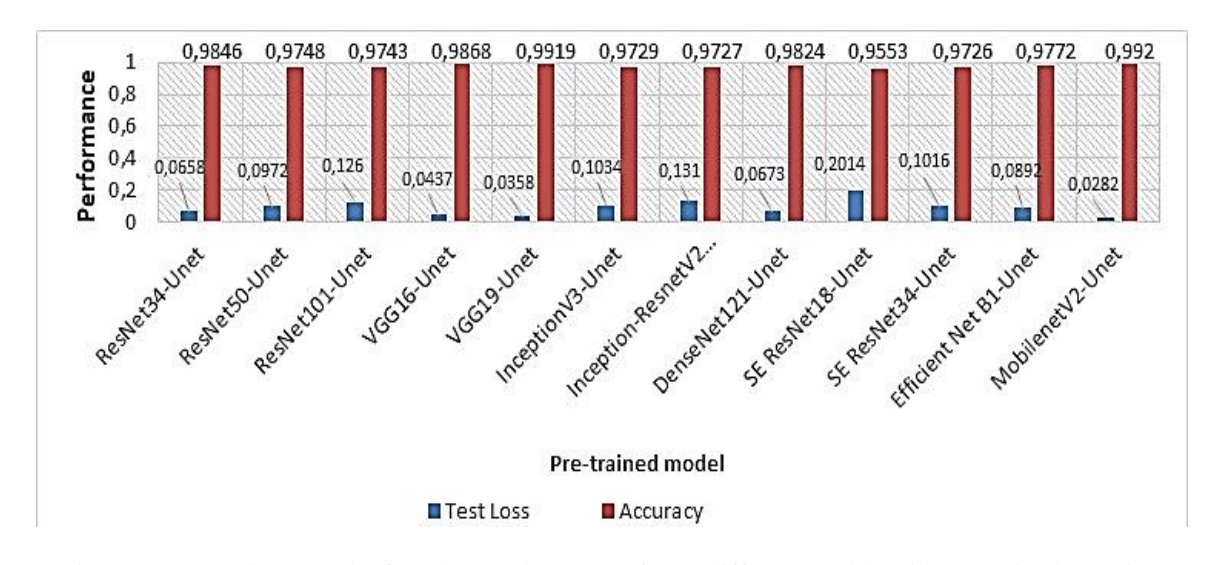


Figure 6. Comparison graph of test loss and accuracy for 12 different models with pre-trained encoders

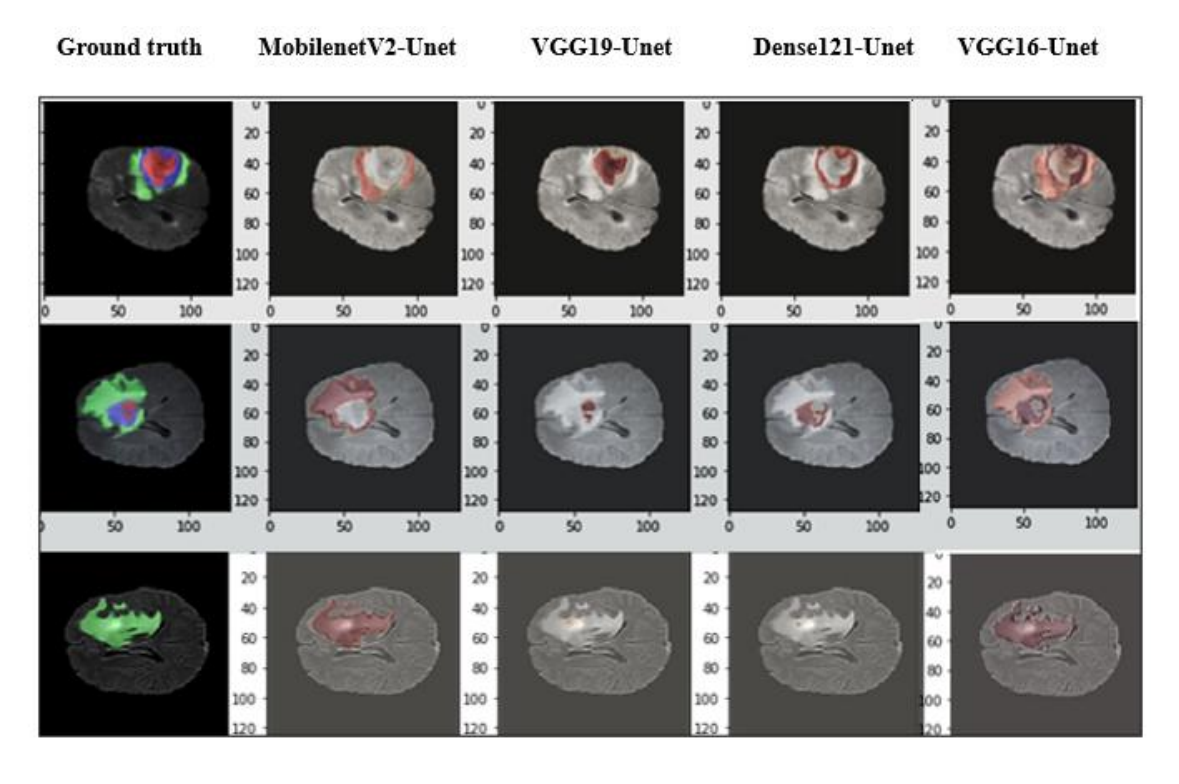


Figure 7. The top four models with pre-trained encoders achieved visual segmentation

Table 3. Previous work in comparison with the MobilenetV2 encoder with U-net models in terms of Jaccard and Dice coefficients for ET, TC, and WT

Model	Jaccard (%)	ET (%)	TC (%)	WT (%)
ResNet34- Unet [20]	63.56	73.96	78.66	82.33
ResNet50- Unet [21]	63.42	73.88	78.45	82.02
ResNet101- Unet [22]	61.08	72.32	77.30	81.14
VGG-16 -Unet [23]	72.23	77.57	80.52	84.61
VGG-19 Unet [24]	74.13	77.75	80.63	85.41
InceptionV3-Unet [12]	70.18	75.77	79.09	83.48
Inception-ResnetV2-Unet [25]	64.58	74.85	78.45	82.45
DenseNet121-Unet [26]	62.09	75.88	79.26	83.61
SE ResNet18-Unet	60.61	72.06	76.49	81.00
SE ResNet34-Unet	62.50	72.57	77.64	82.02
Efficient Net B1-Unet [11]	81.63	79.23	83.57	88.65
MobilenetV2-Unet (this work)	83.45	81.93	86.07	90.3

4. CONCLUSION

This article investigated the efficacy of employing pre-trained transfer learning models as encoders within the U-Net design for segmenting brain tumors. We evaluated twelve pre-trained encoders, initialized with ImageNet weights, using the BraTS 2019 dataset under identical hyperparameter configurations. This study extends the understanding of advanced backbone networks for semantic segmentation, specifically addressing challenges related to interpretability, computational demands, and overfitting. Our comparative analysis, focusing on metrics such as Dice coefficient, test loss, accuracy, and training duration, revealed that the hybrid U-Net model employing MobileNetV2 in the encoding path exhibits superior performance.

The MobileNetV2-enhanced U-Net reached a test accuracy of 99.3%, a cross-validation accuracy of 99%, a Jaccard coefficient of 83.45%, and a test loss of 0.0282. Furthermore, it demonstrated powerful segmentation performance across tumor sub-regions, with Dice coefficients of 86.07% for the TC, 90.3% for the WT, and 81.93% for the ET. Importantly, the MobileNetV2 encoder's lightweight nature translates to reduced computational resource consumption.

According to these results, incorporating MobileNetV2 as an encoder into the U-Net architecture provides a strong argument for precise and effective brain tumor segmentation. This has significant implications for clinical practice, potentially enabling faster and more precise diagnoses, which can lead to enhanced clinical outcomes and informed treatment decision-making. The main limitation of pre-trained models are often complex and large, requiring significant computational resources for fine-tuning, which can be challenging for researchers or practitioners with limited access to advanced computing resources. But the reduced computational cost associated with MobileNetV2 also makes this approach more accessible for resource-constrained environments.

Future research could investigate further optimizing the architecture, perhaps through the incorporation of attention mechanisms or novel loss functions, which could lead to even greater improvements in segmentation performance. Furthermore, future work could involve the adoption of the MobileNetV2-enhanced U-Net framework for additional medical image segmentation requirements, like organ or tumor segmentation. Future research could also benefit from examining the effectiveness of the model in actual time clinical settings and with larger brain datasets.

FUNDING INFORMATION

Authors state no funding involved.

CONFLICT OF INTEREST STATEMENT

Authors state no conflict of interest.

DATA AVAILABILITY

Data availability does not apply to this paper as no new data were created or analyzed in this study.

REFERENCES

- [1] A. H. Saka *et al.*, "Cancer statistics for African American and black people, 2025," *CA: A Cancer Journal for Clinicians*, vol. 75, no. 2, pp. 111–140, Feb. 2025, doi: 10.3322/caac.21874.
- [2] C. Toader *et al.*, "Low-grade gliomas: histological subtypes, molecular mechanisms, and treatment strategies," *Brain Sciences*, vol. 13, no. 12, p. 1700, Dec. 2023, doi: 10.3390/brainsci13121700.

858 🗖 ISSN: 2502-4752

[3] C. Steenhout, L. Deprez, R. Hustinx, and N. Withofs, "Brain tumor assessment: integrating PET/computed tomography and MR imaging modalities," PET Clinics, vol. 20, no. 1, pp. 165–174, Jan. 2025, doi: 10.1016/j.cpet.2024.09.003.

- [4] Y. Li, S. Jiang, Z. Yang, L. Wang, Z. Liu, and Z. Zhou, "Segmentation of brain tumor resections in intraoperative 3D ultrasound images using a semisupervised cross nnSU-Net," *International Journal of Imaging Systems and Technology*, vol. 35, no. 1, Jan. 2025, doi: 10.1002/ima.70018.
- [5] S. Saifullah, R. Dreżewski, A. Yudhana, M. Wielgosz, and W. Caesarendra, "Modified U-Net with attention gate for enhanced automated brain tumor segmentation," *Neural Computing and Applications*, vol. 37, no. 7, pp. 5521–5558, Jan. 2025, doi: 10.1007/s00521-024-10919-3.
- [6] K. V. Shiny, "Brain tumor segmentation and classification using optimized U-Net," *Imaging Science Journal*, vol. 72, no. 2, pp. 204–219, May 2024, doi: 10.1080/13682199.2023.2200614.
- [7] M. M. Taye, "Theoretical understanding of convolutional neural network: concepts, architectures, applications, future directions," Computation, vol. 11, no. 3, p. 52, Mar. 2023, doi: 10.3390/computation11030052.
- [8] A. Hosna, E. Merry, J. Gyalmo, Z. Alom, Z. Aung, and M. A. Azim, "Transfer learning: a friendly introduction," *Journal of Big Data*, vol. 9, no. 1, Oct. 2022, doi: 10.1186/s40537-022-00652-w.
- [9] A. Nawaz, U. Akram, A. A. Salam, A. R. Ali, A. Ur Rehman, and J. Zeb, "VGG-UNET for brain tumor segmentation and ensemble model for survival prediction," in 2021 International Conference on Robotics and Automation in Industry, ICRAI 2021, Oct. 2021, pp. 1–6, doi: 10.1109/ICRAI54018.2021.9651367.
- [10] S. Ghosh, A. Chaki, and K. Santosh, "Improved U-Net architecture with VGG-16 for brain tumor segmentation," *Physical and Engineering Sciences in Medicine*, vol. 44, no. 3, pp. 703–712, May 2021, doi: 10.1007/s13246-021-01019-w.
- [11] S. Y. Lin and C. L. Lin, "Brain tumor segmentation using U-Net in conjunction with EfficientNet," *PeerJ Computer Science*, vol. 10, p. e1754, Jan. 2024, doi: 10.7717/peerj-cs.1754.
- [12] S. F. Rabby, M. A. Arafat, and T. Hasan, "BT-Net: An end-to-end multi-task architecture for brain tumor classification, segmentation, and localization from MRI images," *Array*, vol. 22, p. 100346, Jul. 2024, doi: 10.1016/j.array.2024.100346.
- [13] S. Saifullah and R. Dreżewski, "Brain tumor segmentation using ensemble CNN-transfer learning models: DeepLabV3plus and ResNet50 approach," in *Lecture Notes in Computer Science (including subseries Lecture Notes in Artificial Intelligence and Lecture Notes in Bioinformatics)*, vol. 14835 LNCS, Springer Nature Switzerland, 2024, pp. 340–354.
- [14] R. Preetha, M. Jasmine Pemeena Priyadarsini, and J. S. Nisha, "Brain tumor segmentation using multi-scale attention U-Net with EfficientNetB4 encoder for enhanced MRI analysis," *Scientific Reports*, vol. 15, no. 1, Mar. 2025, doi: 10.1038/s41598-025-94267-9.
- [15] H. Reza, N. I. Tareq, M. M. F. Rabbi, S. A. Tanim, R. A. M. Rudro, and K. Nur, "Acute lymphoblastic leukemia diagnosis and subtype segmentation in blood smears using CNN and U-Net," *Indonesian Journal of Electrical Engineering and Computer Science*, vol. 38, no. 2, p. 950, May 2025, doi: 10.11591/ijeecs.v38.i2.pp950-959.
- [16] W. Weng and X. Zhu, "INet: convolutional networks for biomedical image segmentation," *IEEE Access*, vol. 9, no. 234–241, pp. 16591–16603, 2021, doi: 10.1109/ACCESS.2021.3053408.
- [17] "Brain_Tumor_Segmentation_BraTS_2019," BraTS2019, 2019. https://www.kaggle.com/datasets/aryashah2k/brain-tumor-segmentation-brats-2019.
- [18] Z. Zhang, "Improved adam optimizer for deep neural networks," in 2018 IEEE/ACM 26th International Symposium on Quality of Service, IWQoS 2018, Jun. 2019, pp. 1–2, doi: 10.1109/IWQoS.2018.8624183.
- [19]. Usha Ruby Dr.A, "Binary cross entropy with deep learning technique for Image classification," *International Journal of Advanced Trends in Computer Science and Engineering*, vol. 9, no. 4, pp. 5393–5397, Aug. 2020, doi: 10.30534/ijatcse/2020/175942020.
- [20] J. L. Arrastia et al., "Deeply supervised unet for semantic segmentation to assist dermatopathological assessment of basal cell carcinoma," *Journal of Imaging*, vol. 7, no. 4, p. 71, Apr. 2021, doi: 10.3390/jimaging7040071.
- [21] S. Lefkovits and L. Lefkovits, "U-Net architecture variants for brain tumor segmentation of histogram corrected images," Acta Universitatis Sapientiae, Informatica, vol. 14, no. 1, pp. 49–74, Aug. 2022, doi: 10.2478/ausi-2022-0004.
- [22] S. K. H. Islam, J. Pradhan, P. Vashistha, A. P. Singh, and A. Kishore, "ResNet-CPDS: colonoscopy polyp detection and segmentation using modified ResNet101V2," in *Lecture Notes in Networks and Systems*, vol. 963, Springer Nature Singapore, 2024, pp. 93–105.
- [23] S. Kadry, E. Verdú, R. Damasevicius, L. Abualigah, V. Singh, and V. Rajinikanth, "CNN segmentation of skin melanoma in pre-processed dermoscopy images," *Procedia Computer Science*, vol. 235, pp. 2775–2782, 2024, doi: 10.1016/j.procs.2024.04.262.
- [24] M. A. Khan et al., "VGG19 network assisted joint segmentation and classification of lung nodules in CT images," Diagnostics, vol. 11, no. 12, p. 2208, Nov. 2021, doi: 10.3390/diagnostics11122208.
- [25] V. Rangannavar, S. Mudavi, P. Shavi, N. Patil, S. Itagalli, and N. Yaligar, "Automated gastrointestinal tract image segmentation," in 2024 5th International Conference for Emerging Technology, INCET 2024, May 2024, pp. 1–6, doi: 10.1109/INCET61516.2024.10593285.
- [26] N. Cinar, A. Ozcan, and M. Kaya, "A hybrid DenseNet121-UNet model for brain tumor segmentation from MR images," Biomedical Signal Processing and Control, vol. 76, p. 103647, Jul. 2022, doi: 10.1016/j.bspc.2022.103647.

BIOGRAPHIES OF AUTHORS



П







Aziza I. Hussein received her Ph.D. degree in Electrical & Computer Engineering from Kansas State University, USA, in 2001 and her M.Sc. and B.Sc. degrees from Assiut University, Egypt, in 1989 and 1983, respectively. She joined Effat University in Saudi Arabia in 2004 and established the first Electrical and Computer Engineering program for women in the country and taught related courses. She was the head of the Electrical and Computer Engineering Department at Effat University from 2007-2010. She was the head of the Computer and Systems Engineering Department, Faculty of Engineering, Minia University, Egypt, from 2011-2016. She was a professor and chair of the Electrical & Computer Engineering Department and director of the Master of Energy program at Effat University Saudi Arabia from 2016-2021. Currently, she is a professor and researcher at the same department. Her research interests include microelectronics, analog/digital VLSI system design, RF circuit design, high-speed analog-to-digital converters design, and wireless communications systems design. She can be contacted at email: azibrahim@effatuniversity.edu.sa.



Lamya Gaber D S In 2014, she joined the Department of Computer and Systems Engineering, Minia University, Egypt as a teaching assistant, and since 2023, she has been an assistant professor. Her research interests include test pattern generation, formal verification, parallel programming, and high-performance computing. She can be contacted at email: lamya.gaber@mu.edu.eg.



Mohamed Mourad Mabrook © S received his B.Sc. and M.Sc. degrees in Electrical and Communication Engineering from Assiut University, Egypt, in 2008 and 2013, respectively. He received a Ph.D. degree in the Communication Dept., Menia University, Egypt in 2017. He is an Assistant Professor at Space Communication Engineering Dept in the faculty of Navigation Science and Space Technology (NSST), Beni-Suef University, Beni-Suef, Egypt. Head of Applied Sciences of Space and navigation Program Science 2021. He is a part-time Assistant prof. at Faculty of Engineering, Nahda University (NUB), Beni-Suef, Egypt. He published more than 30 journal and conference papers in the fields of wireless communications, 5G networks, cognitive radio, Artificial intelligence, circuit design, and sensors. He is a reviewer in many international journals related to Elsevier, Springer, and IEEE Publishers. He can be contacted at email: mohamedmourad2008@gmail.com or mohamed.mourad@nsst.bsu.edu.eg.